Functional MRI brain state occupancy in the presence of cerebral small vessel disease – a pre-registered replication analysis of the Hamburg City Health Study

Thies Ingwersen, MD [1], **Carola Mayer, PhD** [1], **Marvin Petersen, MD** [1], **Benedikt M. Frey, MD** [1], **Jens Fiehler, MD** [2], **Uta Hanning, MD** [2], **Simone Kühn, PhD** [3,4], **Jürgen Gallinat, MD** [3], **Raphael Twerenbold, MD** [5], **Christian Gerloff, MD** [6], **Bastian Cheng, MD** [1], **Götz Thomalla, MD** [1], **Eckhard Schlemm, MBBS PhD** [1]

[1]Department of Neurology, University Medical Center Hamburg-Eppendorf; [2]Department of Neuroradiology, University Medical Center Hamburg-Eppendorf; [3]Department of Psychiatry, University Medical Center Hamburg-Eppendorf; [4]Max-Planck-Institut für Bildungsforschung, Berlin; [5]Department of Cardiology, University Medical Center Hamburg-Eppendorf; [6]University Medical Center Hamburg-Eppendorf

✉ **For correspondence:**
e.schlemm@uke.de

Present address:
Dr. Dr. Eckhard Schlemm, Klinik und Poliklinik für Neurologie, Universitätsklinikum Hamburg-Eppendorf, Martinistr. 52, D-20251 Hamburg

Abstract

Objective: To replicate recent findings on the association between the extent of cerebral small vessel disease (cSVD), functional brain network dedifferentiation, and cognitive impairment.

Methods: We analyzed demographic, imaging, and behavioral data from the

prospective population-based Hamburg City Health Study. Using a fully prespecified analysis pipeline, we estimated discrete brain states from structural and resting-state functional magnetic resonance imaging (MRI). In a multiverse analysis, we varied brain parcellations and functional MRI confound regression strategies. The severity of cSVD was operationalized as the volume of white matter hyperintensities of presumed vascular origin. Processing speed and executive dysfunction were quantified using the Trail Making Test (TMT).

Hypotheses: We hypothesized a) that a greater volume of supratentorial white matter hyperintensities would be associated with less time spent in functional MRI-derived brain states of high fractional occupancy; and b) that less time spent in these high-occupancy brain states is associated with a longer time to completion in part B of the TMT.

Results: High-occupancy brain states were characterized by activation or suppression of the default mode network. Every 5.1-fold increase in WMH volume was associated with a 0.94-fold reduction in the odds of occupying DMN-related brain states (P 5.01×10^{-8}). Every 5% increase in time spent in high-occupancy brain states was associated with a 0.98-fold reduction in the TMT-B completion time (P 0.0116). Findings were robust across most brain parcellations and confound regression strategies.

Conclusion: We successfully replicated previous findings on the association between cSVD, functional brain occupancy, and cognition in an independent sample. The data provide further evidence for a functional network dedifferentiation hypothesis of cSVD-related cognitive impairment. Further research is required to elucidate the mechanisms underlying these associations.

Introduction

Cerebral small vessel disease (cSVD) is an arteriolopathy of the brain associated with age and common cardiovascular risk factors (Wardlaw, C. Smith, and Dichgans, 2013). cSVD predisposes patients to ischemic stroke (in particular lacunar stroke) and may lead to cognitive impairment and dementia (Cannistraro et al., 2019). Neuroimaging findings in cSVD reflect its underlying pathology (Wardlaw, Valdés Hernández, and Muñoz-Maniega, 2015) and include white matter hyperintensities (WMH), lacunes of presumed vascular origin, small subcortical infarcts and microbleeds, enlarged perivascular spaces as well

as brain atrophy (Wardlaw, E. E. Smith, et al., 2013). However, the extent of visible cSVD features on magnetic resonance imaging (MRI) is an imperfect predictor of the severity of clinical sequelae (Das et al., 2019) and our understanding of the causal mechanisms linking cSVD-associated brain damage to clinical deficits remains limited (Bos et al., 2018).

Recent efforts have focused on exploiting network aspects of the structural (Tuladhar, Dijk, et al., 2016; Tuladhar, Tay, et al., 2020; Lawrence, Zeestraten, et al., 2018) and functional (Dey et al., 2016; Schulz et al., 2021) organization of the brain to understand the relationship between cSVD and clinical deficits in cognition and other domains that rely on distributed processing. Reduced structural network efficiency has repeatedly been described as a causal factor in the development of cognitive impairment, particularly executive dysfunction and reduced processing speed in cSVD (Lawrence, Chung, et al., 2014; Shen et al., 2020; Reijmer et al., 2016; Prins et al., 2005). Findings with respect to functional connectivity (FC), however, are more heterogeneous than their SC counterparts, perhaps because FC measurements are prone to be affected by hemodynamic factors and noise, resulting in relatively low reliability, especially with resting-state scans of short duration (Laumann, Gordon, et al., 2015). This problem is exacerbated in the presence of cSVD and worsened by arbitrary processing choices (Lawrence, Tozer, et al., 2018; Gesierich et al., 2020).

As a promising new avenue, time-varying, or dynamic, functional connectivity approaches have recently been explored in patients with subcortical ischemic vascular disease (Yin et al., 2022; Xu et al., 2021). Although the study of dynamic FC measures may not solve the problem of limited reliability, especially in small populations or ~~subjects~~ participants with extensive structural brain changes, it adds another – temporal – dimension to the study of functional brain organization, which is otherwise overlooked. Importantly, FC dynamics not only reflect moment-to-moment fluctuations in cognitive processes, but are also related to brain plasticity and homeostasis (Laumann and Snyder, 2021; Laumann, Snyder, et al., 2017), which may be impaired in cSVD.

In the present paper, we aimed to replicate and extend the main results of (Schlemm et al., 2022). In this recent study, the authors analyzed MR imaging and clinical data from the prospective Hamburg City Health Study (HCHS, (Jagodzinski et al., 2020)) using a coactivation pattern approach to define discrete brain states and found associations between the WMH load, time spent in high-occupancy brain states characterized by activation or suppression of the default mode network (DMN), and cognitive impairment. Specifically,

89 every 4.7-fold increase in WMH volume was associated with a 0.95-fold reduction in the

90 odds of occupying a DMN-related brain state; every 2.5 seconds (i.e., one repetition time)

91 not spent in one of those states was associated with a 1.06-fold increase in TMT-B com-

92 pletion times.

93   The fractional occupancy of a functional MRI-derived discrete brain state is a ~~subject-specific~~

94 participant-specific measure of brain dynamics and is defined as the proportion of BOLD

95 volumes assigned to that state relative to all BOLD volumes acquired during a resting-

96 state scan.

97   Our primary hypothesis for the present work was that the volume of supratentorial

98 white matter hyperintensities is associated with fractional occupancy of DMN-related

99 brain states in a middle-aged to elderly population mildly affected by cSVD. Our sec-

100 ondary hypothesis was that fractional occupancy is associated with executive dysfunc-

101 tion and reduced processing speed, measured as the time to complete part B of the Trail

102 Making Test (TMT).

103   Both hypotheses were tested in an independent subsample of the HCHS study popu-

104 lation using the same imaging protocols, examination procedures, and analysis pipelines

105 as those in (Schlemm et al., 2022). The robustness of the associations was explored using

106 a multiverse approach by varying key steps in the analysis pipeline.

Methods

107

Study population

108

109 This study analyzed data from the Hamburg City Health Study (HCHS), an ongoing prospec-

110 tive, population-based cohort study aiming to recruit a cross-sectional sample of 45 000

111 adult participants from the city of Hamburg, Germany (Jagodzinski et al., 2020). From

112 the first 10 000 participants of the HCHS, we planned to include those who were docu-

113 mented to have received brain imaging (n=2648) and exclude those who were analyzed

114 in our previous report (Schlemm et al., 2022) (n=970). The ethical review board of the

115 Landesärztekammer Hamburg (State of Hamburg Chamber of Medical Practitioners) ap-

116 proved the HCHS (PV5131), and all participants provided written informed consent.

Demographic and clinical characterization

117

118 From the study database, we extracted the participants' age at the time of inclusion in

119 years, their sex, and the number of years spent in education. During the visit to the study

center, participants underwent cognitive assessment using standardized tests. From the database, we extracted their performance scores on the Trail Making Test part B, measured in seconds, as an operationalization of executive function and psychomotor processing speed (Tombaugh, 2004; Arbuthnott and Frank, 2000). For descriptive purposes, we also extracted data on past medical history and reported the proportion of participants with a previous diagnosis of dementia.

MRI acquisition and preprocessing

The magnetic resonance imaging protocol for the HCHS includes structural and resting-state functional sequences. The acquisition parameters for a $3\,\mathrm{T}$ Siemens Skyra MRI scanner (Siemens, Erlangen, Germany) have been previously reported (Petersen et al., 2020; Frey et al., 2021) and are given as follows:

For T_1-weighted anatomical images, a 3D rapid acquisition gradient-echo sequence (MPRAGE) was used with the following sequence parameters: repetition time TR = $2500\,\mathrm{ms}$, echo time TE = $2.12\,\mathrm{ms}$, 256 axial slices, slice thickness ST = $0.94\,\mathrm{mm}$, and in-plane resolution IPR = $(0.83 \times 0.83)\,\mathrm{mm}^2$.

T_2-weighted fluid attenuated inversion recovery (FLAIR) images were acquired with the following sequence parameters: TR = $4700\,\mathrm{ms}$, TE = $392\,\mathrm{ms}$, 192 axial slices, ST = $0.9\,\mathrm{mm}$, IPR = $(0.75 \times 0.75)\,\mathrm{mm}^2$.

125 resting state functional MRI volumes were acquired (TR = $2500\,\mathrm{ms}$; TE = $25\,\mathrm{ms}$; flip angle = 90°; slices = 49; ST = $3\,\mathrm{mm}$; slice gap = $0\,\mathrm{mm}$; IPR = $(2.66 \times 2.66)\,\mathrm{mm}^2$). The ~~subjects~~ participants were asked to keep their eyes open and to think of nothing.

We verified the presence and voxel dimensions of expected MRI data for each participant and excluded those for whom at least one of T_1-weighted, FLAIR, and resting-state MRI was missing. We also excluded participants with neuroradiologically confirmed space-occupying intra-axial lesion. To ensure reproducibility, no visual quality assessment of raw images was performed.

For the remaining participants, structural and resting-state functional MRI data was preprocessed using FreeSurfer v6.0 (https://surfer.nmr.mgh.harvard.edu/), and fmriPrep v20.2.6 (Esteban et al., 2019), using default parameters. Participants were excluded if automated processing using at least one of these packages failed.

Quantification of WMH load

151 For our primary analysis, the extent of ischemic white matter disease was operational-
152 ized as the total volume of supratentorial WMHs obtained from automated segmentation
153 using a combination of anatomical priors, BIANCA (Griffanti, Zamboni, et al., 2016), and
154 LOCATE (Sundaresan et al., 2019), post-processed with a minimum cluster size of 30 vox-
155 els, as described in (Schlemm et al., 2022). In an exploratory analysis, we partitioned
156 voxels identified as WMH into deep and periventricular components according to their
157 distance to the ventricular system (cut-off $10\,\mathrm{mm}$, (Griffanti, Jenkinson, et al., 2018))

Brain state estimation

159 The output from fMRIprep was post-processed using xcpEngine v1.2.3 to obtain de-confounded
160 spatially averaged BOLD time series (Ciric, Wolf, et al., 2017). For the primary analysis, we
161 used the *36p* regression strategy and the Schaefer-400 parcellation (Schaefer et al., 2018),
162 as in (Schlemm et al., 2022).

163 Different atlases and confound regression strategies, as implemented in xcpEngine,
164 were included in an exploratory multiverse analysis.

165 Co-activation pattern (CAP) analysis was performed by first aggregating parcellated,
166 de-confounded BOLD signals into a $\left(n_{\mathrm{parcels}} \times \sum_i n_{\mathrm{time\ points},i}\right)$ feature matrix, where $n_{\mathrm{time\ points},i}$
167 denotes the number of retained volumes for ~~subject~~ participant i after confound regres-
168 sion. Clustering was performed using the k-means algorithm ($k = 5$) with a distance mea-
169 sure given by 1 minus the sample Pearson correlation between points, as implemented
170 in Matlab R2021a. We estimated the ~~subject-~~ participant- and state-specific fractional oc-
171 cupancies, which are defined as the proportion of BOLD volumes assigned to each brain
172 state (Vidaurre et al., 2018). The two states with the highest average occupancies were
173 identified as the basis for further analysis.

Statistical analysis

175 For demographic (age, sex, and years of education) and clinical (TMT-B) variables, the
176 number of missing items is reported. For non-missing values, we provide descriptive
177 summary statistics using median and interquartile range. The proportions of men and
178 women in the sample are reported. Since we expected based on our pilot data (Schlemm
179 et al., 2022) that the proportion of missing data would be small, primary regression mod-
180 elling was carried out as a complete-case analysis.

As an outcome-neutral quality check of the implementation of the MRI processing pipeline, brain state estimation, and co-activation pattern analysis, we compared fractional occupancies between brain states. We expected that the average fractional occupancy in the two high-occupancy states would be higher than the average fractional occupancy in the other three states. Point estimates and 95% confidence intervals are presented for the difference in average fractional occupancy to verify this assertion.

For further analyses, non-zero WMH volumes were subjected to logarithmic transformation. Zero values retained their value of zero; to compensate, all models included a binary indicator for zero WMH volume if at least one non-zero WMH value was present.

To assess the primary hypothesis of a negative association between the extent of ischemic white matter disease and time spent in high-occupancy brain states, we performed a fixed-dispersion Beta regression to model the logit of the conditional expectation of the average fractional occupancy of two high-occupancy states as an affine function of the logarithmized WMH load. Age and sex were included as covariates. The strength of the association was quantified as the odds ratio per interquartile ratio of the WMH burden distribution, and is accompanied by a 95% confidence interval. Significance testing of the null hypothesis of no association was conducted at the conventional significance level of 0.05. Estimation and testing were carried out using the 'betareg' package v3.1.4 in R v4.2.1.

To assess the secondary hypothesis of an association between time spent in high-occupancy brain states and executive dysfunction, we performed a generalized linear regression with a Gamma response distribution to model the logarithm of the conditional expected completion time in part B of the TMT as an affine function of the average fractional occupancy of two high-occupancy states. Age, sex, years of education, and logarithmized WMH load were included as covariates. The strength of the association was quantified as a multiplicative factor per percentage point and accompanied by a 95% confidence interval. Significance testing of the null hypothesis of no association was conducted at the conventional significance level of 0.05. Estimation and testing were performed using the glm function included in the 'stats' package from R v4.2.1.

Pre-registered analyses

The analysis plan was ~~pre-restistered~~ pre-registered on June 27 2023 at https://osf.io/fcqmb. The sample size calculation was based on an effect size on the odds ratio scale of 0.95, corresponding to an absolute difference in the probability of occupying a DMN-
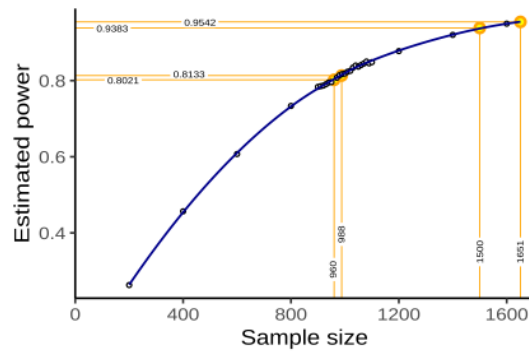
Figure 1 | **Sample size and power estimation.** A-priori estimated power for different sample sizes was obtained as the proportion of synthetic data sets in which the null hypothesis of no association between WMH volume and time spent in high-occupancy brain states an be rejected at the $\alpha = 0.05$ significance level. Proportions are based on a total of $10\,000$ synthetic data sets obtained by bootstrapping the data presented in (Schlemm et al., 2022). Highlighted in orange are the smallest sample size ensuring a power of at least $80\,\%$ ($n = 960$), the sample size of the pilot data ($n = 988$, post-hoc power $81.3\,\%$), the expected sample sample size for this replication study ($n = 1500$, a-priori power $93.9\,\%$), and the achieved sample size ($n = 1651$, a-priori power $95.4\,\%$).

related brain state between the first and third WMH-load quartile of 1.3 percentage points, and between the 5% and 95% percentile of 3.1 percentage points. Approximating half the difference in fractional occupancy of DMN-related states between different task demands (rest vs n-back) in healthy ~~subjects~~participants, which was estimated to lie between 6 and 7 percentage points (Cornblath et al., 2020), this value represented a plausible choice for the smallest effect size of theoretical and practical interest. It also equals the estimated effect size based on the data presented in (Schlemm et al., 2022).

Simple bootstrapping was used to create $10\,000$ hypothetical datasets of size 200, 400, 600, 800, 900, 910, …, 1090, 1100, 1200, 1400, 1500, and 1600. Each dataset was then subjected to the estimation procedure described above. For each sample size, the proportion of datasets in which the primary null hypothesis of no association between fractional occupancy and WMH load could be rejected at $\alpha = 0.05$ was computed and recorded as a power curve in Figure 1.

A sample size of 960 would have allowed the replication of the reported effect with a power of $80.2\,\%$. We had anticipated a sample size of 1500, which would have yielded a power of $93.9\,\%$.

Multiverse analysis

In both (Schlemm et al., 2022) and our primary replication analysis, we made certain analytical choices in the operationalization of brain states and ischemic white matter disease, namely the use of the *36p* confound regression strategy, the Schaefer-400 parcellation,

234 and a BIANCA/LOCATE-based WMH segmentation algorithm. The robustness of the as-
235 sociation between WMH burden and time spent in high-occupancy states with regard to
236 other choices was explored in a multiverse analysis (Steegen et al., 2016). Specifically, in
237 an exploratory analysis, we estimated brain states from BOLD time series processed ac-
238 cording to a variety of established confound regression strategies and aggregated over
239 different cortical brain parcellations (Table 2, Ciric, Rosen, et al., 2018; Ciric, Wolf, et al.,
240 2017). The extent of cSVD was additionally quantified by the volume of deep and periven-
241 tricular white matter hyperintensities.

242 For each combination of analytical choice of confound regression strategy, parcella-
243 tion, and subdivision of white matter lesion load ($9 \times 9 \times 3 = 243$ scenarios in total), we
244 quantified the association between WMH load and average time spent in high-occupancy
245 brain states using odds ratios and 95% confidence intervals as described above.

246 No hypothesis testing was performed for these multiverse analyses. Rather, they
247 serve to inform about the robustness of the outcome of the test of the primary hypoth-
248 esis. Any substantial conclusions about the association between the severity of cerebral
249 small vessel pathology and the time spent in high-occupancy brain states were drawn
250 from the primary analysis using pre-specified methodological choices, as stated in the
251 Scientific Question in Table 1.

Further exploratory analysis

253 In previous work, two high-occupancy brain states have been related to the default mode
254 network (Cornblath et al., 2020). We further explored this relationship by computing, for
255 each individual brain state, the cosine similarity of the positive and negative activations of
256 the cluster's centroid with a set of a priori defined functional 'communities' or networks
257 (Schaefer et al., 2018; Yeo et al., 2011). The results were visualized as spider plots for the
258 Schaefer atlases.

259 In further exploratory analyses, we describe the associations between brain state dy-
260 namics and other measures of cognitive ability such as memory and language.

Pilot data and analysis

262 Summary data from the first 1000 imaging data points of the HCHS have been published
263 with (Schlemm et al., 2022) and formed the basis for the hypotheses tested in this replication
264 study. Before pregistration, we had implemented our prespecified analysis pipeline described
265 above in R and Matlab, and applied it to this previous sample. Data, code and results

Timeline and access to data

269 At the time of planning of this study, all demographic, clinical and imaging data used in
270 this analysis had been collected by the HCHS and were held in the central trial database.
271 Quality checks for non-imaging variables had been performed centrally. WMH segmentation
272 based on structural MRI data of the first 10 000 participants of the HCHS had been performed
273 previously using the BIANCA/LOCATE approach (Rimmele et al., 2022). Functional MRI
274 data and clinical measures of executive dysfunction (TMT-B scores) had not previously
275 been analyzed by the pre-registering author (ES).

Deviations from preregistration

277 For deconfounding and aggregating BOLD data at brain parcellation level, the software
278 xcpEngine was used in version 1.2.3, not 1.2.1, to ensure that that the correct MNI ref-
279 erence template (MNI152NLin2009cAsym) is used for registration of brain atlases. This
280 decision was made before analysing the data.

Results

282 For this replication study, a total of 2648 datasets were available, of which 970 were al-
283 ready included in our previous analysis and thus discarded. In 13 of the resulting 1678
284 datasets, one or more MRI sequences were missing. Of the complete datasets (n=1665),
285 we excluded 5 participants due to intra-axial space-occupying lesions. An additional 9
286 ~~subjects~~ participants were excluded because of unsuccessful preprocessing, WMH seg-
287 mentation, or xcpEngine failure, resulting in 1651 datasets for analysis. A study-flowchart
288 is provided in Figure 2.

289 Baseline demographic and cognitive values, including the number of missing items,
290 are reported in Table 4.

291 WMH volumes (median 1.05 mL, IQR 0.47 mL to 2.37 mL), motion estimates, and frac-
292 tional occupancies of brain states 1 through 5 are reported in Table 5.

293 In an outcome-neutral quality check of the implementation of (i) the MRI processing
294 pipeline, (ii) brain state estimation, and (iii) co-activation pattern analysis, the mean differ-
295 ence in fractional occupancy between high- and low-occupancy states was consistently
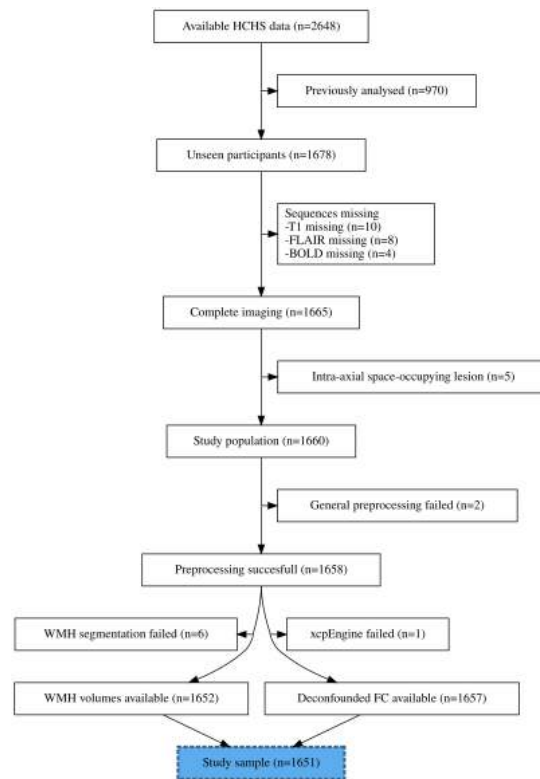
Figure 2 | Study flowchart. Composition of the study population after application of inclusion and exclusion criteria, and image processing.

---

²⁹⁶ maintained, with a point-estimate of the separation between two high-occupancy and
²⁹⁷ three low-occupancy states of $6.7\,\%$ (95 % confidence interval, $6.2\,\%$ to $7.1\,\%$) in the *36p*
²⁹⁸ paradigm. This indicates that the implementation of the pipeline was correct and that
²⁹⁹ the brain state estimation and co-activation pattern analysis worked as intended.

³⁰⁰ Pre-registered hypotheses

³⁰¹ Association between WMH load and fractional occupancy

³⁰² The results of the test of our primary preregistered hypothesis of an association be-
³⁰³ tween supratentorial WMH volume and the time spent in high-occupancy brain states
³⁰⁴ are shown in Figure 3 and Table 7.

³⁰⁵ Adjusted for age and sex, there was a 0.94-fold reduction in the odds of occupying a
³⁰⁶ high-occupancy brain state for every 5.1-fold increase in WMH load (P 5.01×10^{-8}).

³⁰⁷ Association between executive function and fractional occupancy in DMN-
³⁰⁸ related states

³⁰⁹ The results of the test of our secondary preregistered hypothesis of an association be-
³¹⁰ tween time spent in high-occupancy brain states and executive function as measured by
³¹¹ the complete part B of the TMT are shown in Figure 4 and Table 9.

³¹² Adjusted for age, sex, WMH volume, and years of education, there was a 0.98-fold
³¹³ reduction in the time to complete the TMT-B for every 5 % increase in the time spent in
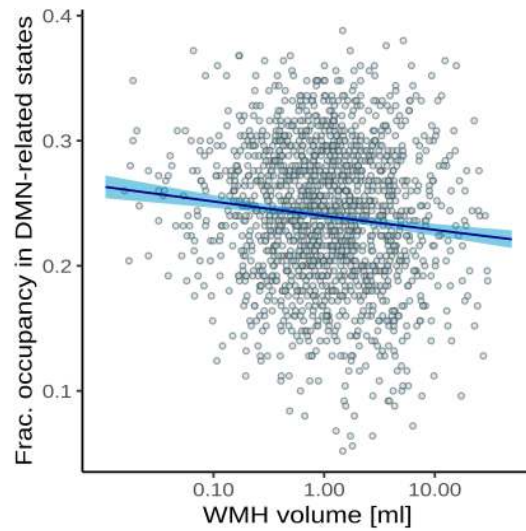
Figure 3 | Association between time spent in high-occupancy brain states and supratentorial WMH volume. Point estimates (black line) and 95%-confidence region (light blue ribbon) of the conditional mean fractional occupancy are obtained from unadjusted beta regression modelling. Each marker represents one of N=1642 independent participants with a non-zero total WMH volume.

Figure 4 | Association between time spent in high-occupancy DMN-related brain states and TMT-B completion time. Point estimates (black line) and 95%-confidence region (light blue ribbon) of the conditional mean TMT-B completion time are obtained from unadjusted Gamma regression modelling. Each marker represent one of N=1482 independent participants with non-zero total WMH volume and available TMT-B data.
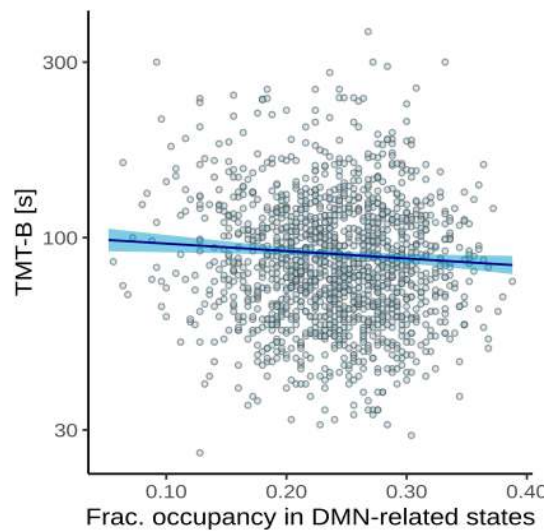
327 icant negative and no significant positive associations, irrespective of operationalization
328 of cSVD (total vs. periventricular vs. deep WMH volume) (Figure 5B).

Additional analyses

Connectivity profiles of brain states – relation to default mode network

331 Based on the cosine similarity between positive and negative activations of cluster cen-
332 troids and indicator vectors of pre-defined large scale brain networks, network activation
333 profiles were computed for brain states estimated from Schaefer parcellations of varying
334 spatial ~~resolution~~resolutions.

335   Figure 6 shows the corresponding spider plots, identifying states characterized by
336 activation (DMN+) or suppression (DMN-) of the default mode network as states with the
337 highest fractional occupancy.

Association with other cognitive domains

339 Associations between the time spent in high-occupancy DMN-related brain states and
340 cognitive measures beyond TMT-B are shown in Figure 7.

341   Adjusted for age, sex, WMH load, and years of education, FO in DMN-related states
342 appeared to be associated with better word recall (~~aOR~~ adjusted OR 1.19, nominal P
343 0.013), but not with global cognitive functioning (MMSE, ~~aOR~~ adjusted OR 1.09) or vocab-
344 ulary (aOR 1.09), nor with verbal fluency (animal naming, adjusted $\exp(\beta)$ 1.04), or pure
345 processing speed (TMT-A, adjusted $\exp(\beta)$ 0.97).

Summary and Discussion

347 In this pre-registered cross-sectional study we replicated the key findings of Schlemm
348 et al., 2022 in an independent population-based sample of 1651 middle-aged to elderly
349 participants of the Hamburg City Health Study.

350   First, we confirmed that the severity of cerebral small vessel disease is associated with
351 the time spent in high-occupancy brain states, defined by functional MRI. More precisely,
352 we showed that every 5.1-fold increase in the volume of supratentorial white matter hy-
353 perintensities of presumed vascular origin (WMH) was associated with a 0.95-fold reduc-
354 tion in the odds of occupying a brain state characterized by activation or suppression of
355 the default-mode network, at any given time during the resting-state scan.

356   Second, we confirmed that the time spent in high-occupancy brain states at rest is
357 associated with cognitive performance. More precisely, a 5%-reduction in the fractional
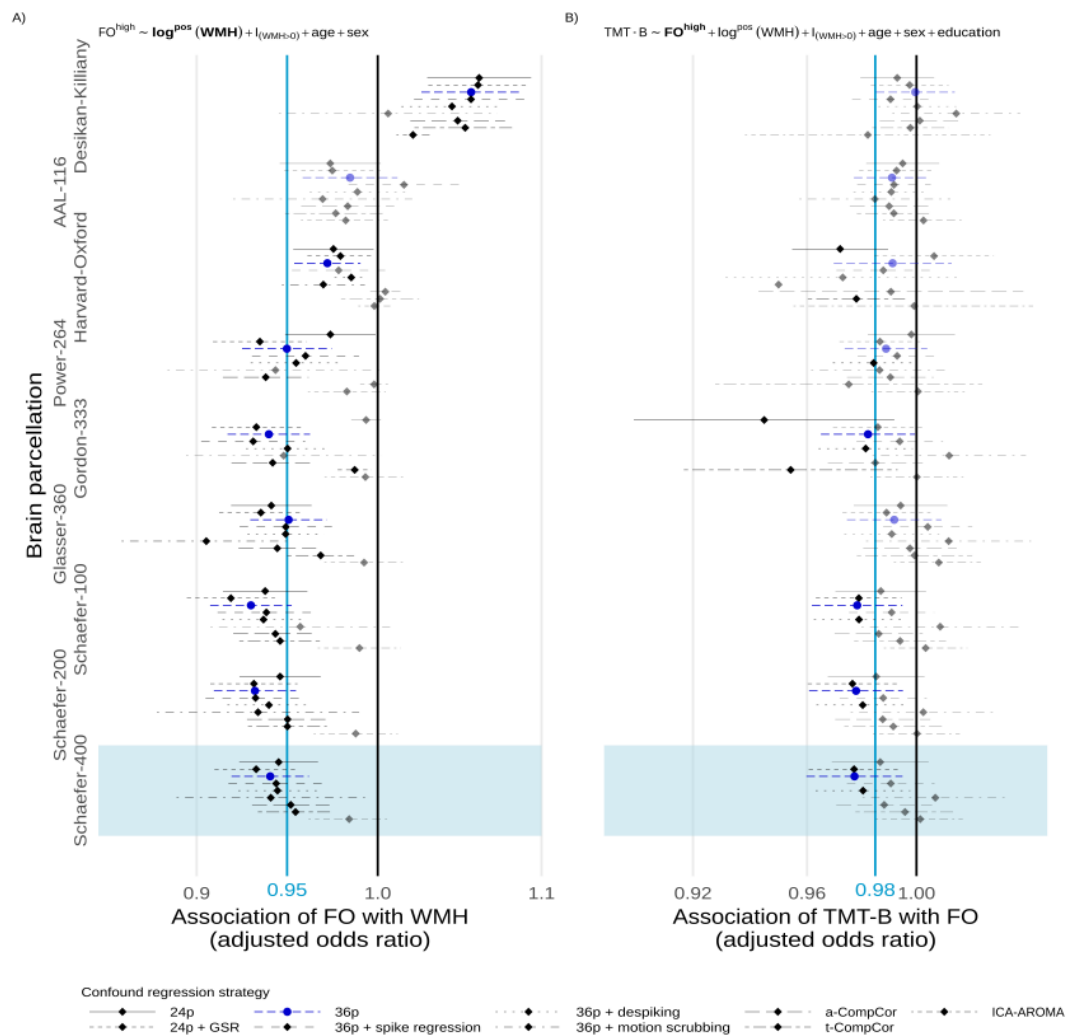
Figure 5 | Multiverse analysis. Adjusted effect size estimates of the associations between cSVD severity (WMH volume) and network dedifferentiation (less time spent in high-occupancy DMN-related brain states) [**A)**], and between network dedifferentiation and executive function (TMT-B completion time) [**B)**]. Effect sizes are given per 5.1-fold increase in WMH volume and a 5%-increase in fractional occupancy, respectively. Markers and line segments indicate point estimates and 95%-confidence intervals for adjusted odds ratios for different combinations of confound regression strategy and brain parcellation. The primary analytical choices are indicated by dark blue circles (36p) and light blue shading (Schaefer-400). Model equations for beta and gamma regressions, respectively, are given at the top. Vertical lines indicate no effect (black) and the effect size observed in the discovery cohort (Schlemm et al., 2022) (light blue), respectively, for reference. Effect sizes not reaching nominal statistical significance ($\alpha = 0.05$) are shown desaturated. Corresponding data based on periventricular and deep WMH volumes are presented in the Supplementary Appendix.
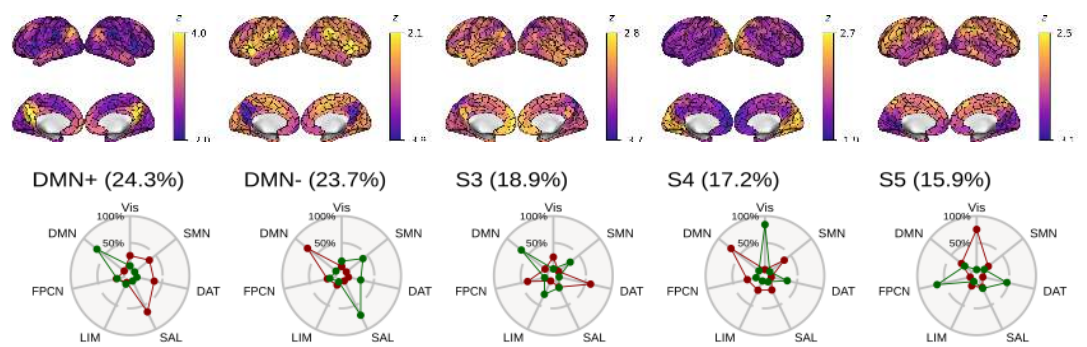
Figure 6 | **Connectivity profiles of brain states.** [**Top**] Centroids of each identified brain state visualized in brain space. Note the individual color scales. [**Bottom**] Cosine similarity between centroids of brain states and signed indicator vectors corresponding to activation (green) and suppression (red) of each of seven predefined large-scale functional brain networks (Yeo et al., 2011).
States are ordered by mean fractional occupancy across N=1651 independent participants, indicated by parenthetical percentages. Two high-occupancy states are characterized by activation or suppression of the DMN, the remaining three low-occupancy states (S3–5) were not used in the present study. Note that mean FO values are similar, but not identical, to median FO values reported in Table 5.

358 occupancy of DMN-related brain states was associated with a 1.02-fold increase in the

359 time to complete part B of the trail making test (TMT).

360 In a pre-planned multiverse analysis, ~~these findings~~ findings relating to our primary

361 and, to a lesser extent, secondary hypotheses were robust with respect to variations in

362 brain parcellations and confound regression strategies. Inconsistent results were found

363 with the Desikan–Killiany parcellation, likely reflecting the notion that the spatial resolu-

364 tion and functional specificity of this coarse, structurally defined atlas are inadequate for

365 analyzing functionally defined brain states. Across brain parcellations, effect sizes were

366 smaller with the ICA-AROMA confound regression strategy and failed to reach nominal

367 statistical significance. This might be due to a relatively large residual motion compo-

368 nent in measures of dynamical functional Connectivity after de-noising with ICA-AROMA,

369 as described previously (Lydon-Staley et al., 2019).

370 We also confirmed across several brain parcellation resolutions that high-occupancy

371 states at rest are characterized by either activation or suppression of the default mode

372 network, reflecting its role as the predominant task-negative brain network.

373 In unplanned, exploratory analyses, we described the association between brain state

374 dynamics and cognitive measures other than executive function and processing speed

375 and reported a strong, preliminary association between time spent in high-occupancy

376 states and delayed word recall.
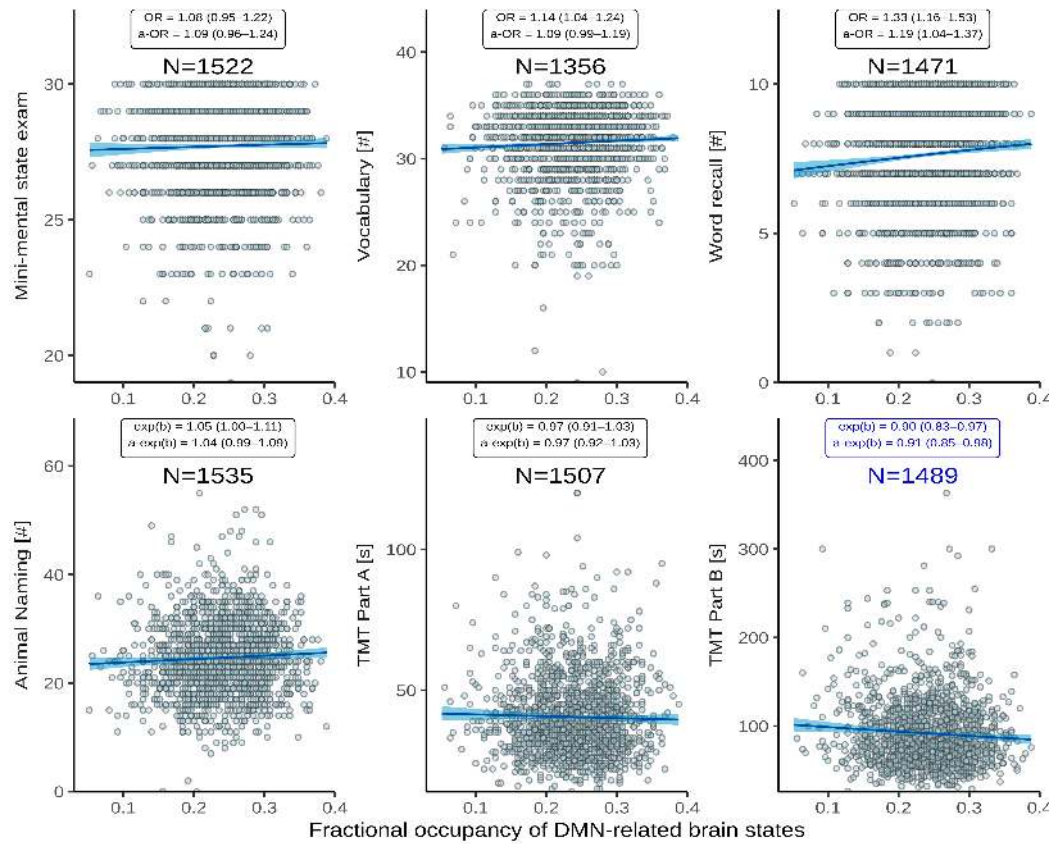
Figure 7 | Association between time spent in high-occupancy DMN-related brain states and cognitive measures. Point estimates (black line) and 95%-confidence region (light blue ribbon) of the conditional mean cognitive measures are obtained from unadjusted binomial (top row: Mini-Mental State Examination, Vocabulary, Word List Recall, logit link) and Gamma regression (bottom row: Animal Naming, Trail Making Test [TMT] A/B: log link) modelling. Each marker represents one of N independent participants, as indicated. Insets report effect sizes and P-values both with (adjusted [a-]) and without adjustment for the nuisance variables age, sex, WMH volume (coded as in Figure 5), and years of education. Effect sizes were quantified as odds ratios (ORs) (top) or response scale multipliers [exp(b)] (bottom), and correspond to a 20%-increase in fractional occupancy. Note the different reference change in FO compared to Table 9 chosen to adequately represent some of the smaller effect sizes. The bottom right panel highlighted in dark blue reproduces Figure 4.

We further explored, ~~but did not report in detail~~and report in the Supplementary appendix, the effect of motion; ~~all reported associations~~ results relating to our primary and, to a lesser extent, secondary, hypotheses were robust to additional, unplanned adjustments for DVARS, RMSD~~or~~, and mean framewise displacement.

The presented results provide robust evidence for a behaviorally relevant association between cerebral small vessel disease and functional brain network dedifferentiation.

Further research is required to replicate our findings in different populations, such as those affected more severely by cSVD or cognitive impairment, or being studied using different imaging protocols, to determine the generalizability of our findings with respect to varying operationalizations of the notions of cSVD, brain state, and cognition, and to understand the mechanisms underlying the reported associations.

~~Timeline and access to data~~

~~At the time of planning of this study, all demographic, clinical and imaging data used in this analysis had been collected by the HCHS and were held in the central trial database. Quality checks for non-imaging variables had been performed centrally. WMH segmentation based on structural MRI data of the first 10 000 participants of the HCHS had been performed previously using the BIANCA/LOCATE approach . Functional MRI data and clinical measures of executive dysfunction (TMT-B scores) had not previously been analyzed by the pre-registering author (ES).~~

Acknowledgment

This preprint was created using the LaPreprint template (https://github.com/roaldarbol/lapreprint) by Mikkel Roald-Arbøl .

Disclosure

The authors of this article declare that they have no financial conflict of interest with the content of this article.

References

Arbuthnott, Katherine and Janis Frank (2000). "Trail making test, part B as a measure of executive control: validation using a set-switching paradigm". In: *Journal of clinical and experimental neuropsychology* 22.4, pp. 518–528.

Behzadi, Yashar et al. (2007). "A component based noise correction method (CompCor) for BOLD and perfusion based fMRI". In: *Neuroimage* 37.1, pp. 90–101.

Bos, Daniel et al. (2018). "Cerebral small vessel disease and the risk of dementia: A systematic review and meta-analysis of population-based evidence". en. In: *Alzheimers. Dement.* 14.11, pp. 1482–1492.

Cannistraro, Rocco J et al. (2019). "CNS small vessel disease: A clinical review". en. In: *Neurology* 92.24, pp. 1146–1156.

Ciric, Rastko, Adon FG Rosen, et al. (2018). "Mitigating head motion artifact in functional connectivity MRI". In: *Nature protocols* 13.12, pp. 2801–2826.

Ciric, Rastko, Daniel H Wolf, et al. (2017). "Benchmarking of participant-level confound regression strategies for the control of motion artifact in studies of functional connectivity". en. In: *Neuroimage* 154, pp. 174–187.

Cornblath, Eli J et al. (2020). "Temporal sequences of brain activity at rest are constrained by white matter structure and modulated by cognitive demands". en. In: *Commun Biol* 3.1, p. 261.

Cox, Robert W (1996). "AFNI: software for analysis and visualization of functional magnetic resonance neuroimages". In: *Computers and Biomedical research* 29.3, pp. 162–173.

Das, Alvin S et al. (2019). "Asymptomatic Cerebral Small Vessel Disease: Insights from Population-Based Studies". en. In: *J. Stroke Cerebrovasc. Dis.* 21.2, pp. 121–138.

Desikan, Rahul S et al. (2006). "An automated labeling system for subdividing the human cerebral cortex on MRI scans into gyral based regions of interest". In: *Neuroimage* 31.3, pp. 968–980.

Dey, Ayan K et al. (2016). "Pathoconnectomics of cognitive impairment in small vessel disease: A systematic review". en. In: *Alzheimers. Dement.* 12.7, pp. 831–845.

Esteban, Oscar et al. (2019). "fMRIPrep: a robust preprocessing pipeline for functional MRI". en. In: *Nat. Methods* 16.1, pp. 111–116.

Frey, Benedikt M et al. (2021). "White matter integrity and structural brain network topology in cerebral small vessel disease: The Hamburg city health study". en. In: *Hum. Brain Mapp.* 42.5, pp. 1406–1415.

Friston, Karl J et al. (1996). "Movement-related effects in fMRI time-series". In: *Magnetic resonance in medicine* 35.3, pp. 346–355.

[438] Gesierich, Benno et al. (2020). "Alterations and test-retest reliability of functional connectivity network measures in cerebral small vessel disease". en. In: *Hum. Brain Mapp.* 41.10, pp. 2629–2641.

[441] Glasser, Matthew F et al. (2016). "A multi-modal parcellation of human cerebral cortex". en. In: *Nature* 536.7615, pp. 171–178.

[443] Gordon, Evan M et al. (2016). "Generation and Evaluation of a Cortical Area Parcellation from Resting-State Correlations". en. In: *Cereb. Cortex* 26.1, pp. 288–303.

[445] Griffanti, Ludovica, Mark Jenkinson, et al. (2018). "Classification and characterization of periventricular and deep white matter hyperintensities on MRI: A study in older adults". en. In: *Neuroimage* 170, pp. 174–181.

[448] Griffanti, Ludovica, Giovanna Zamboni, et al. (2016). "BIANCA (Brain Intensity AbNormality Classification Algorithm): A new tool for automated segmentation of white matter hyperintensities". en. In: *Neuroimage* 141, pp. 191–205.

[451] Jagodzinski, Annika et al. (2020). "Rationale and Design of the Hamburg City Health Study". en. In: *Eur. J. Epidemiol.* 35.2, pp. 169–181.

[453] Laumann, Timothy O, Evan M Gordon, et al. (2015). "Functional system and areal organization of a highly sampled individual human brain". In: *Neuron* 87.3, pp. 657–670.

[455] Laumann, Timothy O and Abraham Z Snyder (2021). "Brain activity is not only for thinking". In: *Current Opinion in Behavioral Sciences* 40, pp. 130–136.

[457] Laumann, Timothy O, Abraham Z Snyder, et al. (2017). "On the stability of BOLD fMRI correlations". In: *Cerebral cortex* 27.10, pp. 4719–4732.

[459] Lawrence, Andrew J, Ai Wern Chung, et al. (2014). "Structural network efficiency is associated with cognitive impairment in small-vessel disease". en. In: *Neurology* 83.4, pp. 304–311.

[462] Lawrence, Andrew J, Daniel J Tozer, et al. (2018). "A comparison of functional and tractography based networks in cerebral small vessel disease". en. In: *Neuroimage Clin* 18, pp. 425–432.

[465] Lawrence, Andrew J, Eva A Zeestraten, et al. (2018). "Longitudinal decline in structural networks predicts dementia in cerebral small vessel disease". en. In: *Neurology* 90.21, e1898–e1910.

[468] Lydon-Staley, David M et al. (2019). "Evaluation of confound regression strategies for the mitigation of micromovement artifact in studies of dynamic resting-state func-

tional connectivity and multilayer network modularity". In: *Network Neuroscience* 3.2, pp. 427–454.

Macey, Paul M et al. (2004). "A method for removal of global effects from fMRI time series". In: *Neuroimage* 22.1, pp. 360–366.

Makris, Nikos et al. (2006). "Decreased volume of left and total anterior insular lobule in schizophrenia". In: *Schizophrenia research* 83.2-3, pp. 155–171.

Muschelli, John et al. (2014). "Reduction of motion-related artifacts in resting state fMRI using aCompCor". In: *Neuroimage* 96, pp. 22–35.

Petersen, Marvin et al. (2020). "Network Localisation of White Matter Damage in Cerebral Small Vessel Disease". en. In: *Sci. Rep.* 10.1, p. 9210.

Power, Jonathan D, Alexander L Cohen, et al. (2011). "Functional network organization of the human brain". en. In: *Neuron* 72.4, pp. 665–678.

Power, Jonathan D, Anish Mitra, et al. (2014). "Methods to detect, characterize, and remove motion artifact in resting state fMRI". In: *Neuroimage* 84, pp. 320–341.

Prins, Niels D et al. (2005). "Cerebral small-vessel disease and decline in information processing speed, executive function and memory". en. In: *Brain* 128.Pt 9, pp. 2034–2041.

Pruim, Raimon HR et al. (2015). "ICA-AROMA: A robust ICA-based strategy for removing motion artifacts from fMRI data". In: *Neuroimage* 112, pp. 267–277.

Reijmer, Yael D et al. (2016). "Small vessel disease and cognitive impairment: The relevance of central network connections". en. In: *Hum. Brain Mapp.* 37.7, pp. 2446–2454.

Rimmele, David Leander et al. (2022). "Association of Carotid Plaque and Flow Velocity With White Matter Integrity in a Middle-aged to Elderly Population". en. In: *Neurology*.

Satterthwaite, Theodore D et al. (2013). "An improved framework for confound regression and filtering for control of motion artifact in the preprocessing of resting-state functional connectivity data". In: *Neuroimage* 64, pp. 240–256.

Schaefer, Alexander et al. (2018). "Local-Global Parcellation of the Human Cerebral Cortex from Intrinsic Functional Connectivity MRI". en. In: *Cereb. Cortex* 28.9, pp. 3095–3114.

Schlemm, Eckhard et al. (2022). "Equalization of Brain State Occupancy Accompanies Cognitive Impairment in Cerebral Small Vessel Disease". en. In: *Biol. Psychiatry* 92.7, pp. 592–602.

Schulz, Maximilian et al. (2021). "Functional connectivity changes in cerebral small vessel disease - a systematic review of the resting-state MRI literature". en. In: *BMC Med.* 19.1, p. 103.

503 Shen, Jun et al. (2020). "Network Efficiency Mediates the Relationship Between Vascular
504 Burden and Cognitive Impairment: A Diffusion Tensor Imaging Study in UK Biobank".
505 en. In: *Stroke* 51.6, pp. 1682–1689.

506 Steegen, Sara et al. (2016). "Increasing Transparency Through a Multiverse Analysis". en.
507 In: *Perspect. Psychol. Sci.* 11.5, pp. 702–712.

508 Sundaresan, Vaanathi et al. (2019). "Automated lesion segmentation with BIANCA: Im-
509 pact of population-level features, classification algorithm and locally adaptive thresh-
510 olding". en. In: *Neuroimage* 202, p. 116056.

511 Tombaugh, Tom N (2004). "Trail Making Test A and B: normative data stratified by age
512 and education". en. In: *Arch. Clin. Neuropsychol.* 19.2, pp. 203–214.

513 Tuladhar, Anil M, Ewoud van Dijk, et al. (2016). "Structural network connectivity and cog-
514 nition in cerebral small vessel disease". en. In: *Hum. Brain Mapp.* 37.1, pp. 300–310.

515 Tuladhar, Anil M, Jonathan Tay, et al. (2020). "Structural network changes in cerebral small
516 vessel disease". en. In: *J. Neurol. Neurosurg. Psychiatry* 91.2, pp. 196–203.

517 Tzourio-Mazoyer, Nathalie et al. (2002). "Automated anatomical labeling of activations in
518 SPM using a macroscopic anatomical parcellation of the MNI MRI single-subject brain".
519 In: *Neuroimage* 15.1, pp. 273–289.

520 Vidaurre, Diego et al. (2018). "Discovering dynamic brain networks from big data in rest
521 and task". en. In: *Neuroimage* 180.Pt B, pp. 646–656.

522 Wardlaw, Joanna M, Colin Smith, and Martin Dichgans (2013). "Mechanisms of sporadic
523 cerebral small vessel disease: insights from neuroimaging". en. In: *Lancet Neurol.* 12.5,
524 pp. 483–497.

525 Wardlaw, Joanna M, Eric E Smith, et al. (2013). "Neuroimaging standards for research
526 into small vessel disease and its contribution to ageing and neurodegeneration". en.
527 In: *Lancet Neurol.* 12.8, pp. 822–838.

528 Wardlaw, Joanna M, Maria C Valdés Hernández, and Susana Muñoz-Maniega (2015). "What
529 are white matter hyperintensities made of? Relevance to vascular cognitive impair-
530 ment". en. In: *J. Am. Heart Assoc.* 4.6, p. 001140.

531 Xu, Yuanhang et al. (2021). "Altered Dynamic Functional Connectivity in Subcortical Is-
532 chemic Vascular Disease With Cognitive Impairment". en. In: *Front. Aging Neurosci.* 13,
533 p. 758137.

534 Yeo, B T Thomas et al. (2011). "The organization of the human cerebral cortex estimated
535 by intrinsic functional connectivity". en. In: *J. Neurophysiol.* 106.3, pp. 1125–1165.

Yin, Wenwen et al. (2022). "The Clustering Analysis of Time Properties in Patients With Cerebral Small Vessel Disease: A Dynamic Connectivity Study". en. In: *Front. Neurol.* 13, p. 913241.

Table 1 | **Study Design Template.** Overview of the Scientific Questions addressed in the present study (first column), the two main hypotheses being investigated (second column), and details of the underlying study.

Question	Hypothesis	Sampling plan	Analysis plan	Rationale for deciding the sensitivity of the test	Interpretation given different outcomes	Theory that could be shown wrong by the outcome
Is severity of cerebral small disease, quantified by the volume of supratentorial white matter hyperintensities of presumed vascular origin (WMH), associated with time spent in high-occupancy brain states, defined by resting-state functional MRI?	**(Primary)** Higher WMH volume is associated with lower average occupancy of the two highest-occupancy brain states.	Available ~~subjects~~ participants with clinical and imaging data from the the HCHS (Jagodzinski et al., 2020)	Standardized preprocessing of structural and functional MRI data • automatic quantification of WMH • co-activation pattern analysis • multivariable generalised regression analyses	Tradition	$P < 0.05$ –> rejection of the null hypothesis of no association between cSVD and fractional occupancy; $P > 0.05$ –> insufficient evidence to reject the null hypothesis	Functional brain dynamics are not related to subcortical ischemic vascular disease.
Is time spent in high-occupancy brain states associated with cognitive impairment, measured as the time to complete part B of the trail making test (TMT)?	**(Secondary)** Lower average occupancy of the two highest-occupancy brain states is associated with longer TMT-B time.	as above	as above	as above	$P < 0.05$ –> rejection of the null hypothesis of no association between fractional occupancy and cognitive impairment; $P > 0.05$ –> insufficient evidence to reject the null hypothesis	Cognitive function is not related to MRI-derived functional brain dynamics.

Name of the atlas	#parcels	Reference
Desikan–Killiany	86	Desikan et al., 2006
AAL	116	Tzourio-Mazoyer et al., 2002
Harvard–Oxford	112	Makris et al., 2006
glasser360	360	Glasser et al., 2016
gordon333	333	Gordon et al., 2016
power264	264	Power, Cohen, et al., 2011
schaefer{N}	100	Schaefer et al., 2018
	200	
	400	

AAL: Automatic Anatomical Labelling

(a) Parcellations

Design	Reference
24p	Friston et al., 1996
24p + GSR	Macey et al., 2004
36p	Satterthwaite et al., 2013
36p + spike regression	Cox, 1996
36p + despiking	Satterthwaite et al., 2013
36p + scrubbing	Power, Mitra, et al., 2014
aCompCor	Muschelli et al., 2014
tCompCor	Behzadi et al., 2007
AROMA	Pruim et al., 2015

GSR: Global signal regression, AROMA: Automatic Removal of Motion Artifacts

(b) Confound regression strategies, adapted from (Ciric, Wolf, et al., 2017)

Table 2 | Multiverse analysis. Overview over different brain parcellations and confound regression strategies implemented using xcpEngine (Ciric, Rosen, et al., 2018). A total of $9 \times 9 = 81$ analytical combinations were explored to assess the robustness of our results with respect to these processing choices.

	N = 1,651
Demographics (no Missing n (%))	
Age, yr	
Median (IQR)	66 (59 – 72)
Sex	
Male	940/1651 (57%)
Female	711/1651 (43%)
Cardiovascular risk factors	
Hypertension	
Present	1177/1611 (73.1%)
Missing n (%)	85 (5.1%)
Diabetes	
Present	157/1566 (10%)
Missing n (%)	40 (2.4%)
Smoking	
Present	200/1360 (14.7%)
Missing n (%)	201 (12.9%%)
Hyperlipidaemia	
Present	426/1578 (27%)
Missing n (%)	73 (4.4%)
Cognitive test results	
MMSE, # (max. 30)	
Median (IQR)	28 (27 – 29)
Missing n (%)	129 (7.8%)
Vocabulary (MWT-B), # (max. 37)	
Median (IQR)	32 (30 – 34)
Missing n (%)	295 (18%)
Word recall, # (max. 10)	
Median (IQR)	8 (6 – 9)
Missing n (%)	180 (11%)
Animal Naming	
Median (IQR)	24 (20 – 29)
Missing n (%)	116 (7.0%)
TMT-A, seconds	
Median (IQR)	38 (31 – 48)
Missing n (%)	144 (8.7%)
TMT-B, seconds	
Median (IQR)	83 (65 – 110)
Missing n (%)	162 (9.8%)
History	
Diagnosed dementia	
Present	6/1645 (0.4%)
Missing n (%)	6 (0.4%)
Years of education	
Median (IQR)	13 (12 – 16)
Missing n (%)	34 (2%)

Table 4 | **Descriptive statistics of the study population.** Data are presented as median (interquartile range) or count (percentage) of non-missing items, as appropriate. Number of percentage of missing items are reported separately.

	N = 1,651
WMH volume[1], mL	
Total	1.05 (0.47 – 2.37), 9 Z
Periventricular	0.94 (0.43 – 2.04), 9 Z
Deep	0.10 (0.03 – 0.37), 344 Z
Motion during rs-fMRI	
Framewise displacement, mm	0.21 (0.15 – 0.63)
RMSD, mm	0.086 (0.058 – 0.12)
DVARS	27.8 (24.3 – 31.8)
Fractional occupancy, %	
DMN+	24.8 (20.8 – 28.0)
DMN-	24.0 (20.0 – 28.0)
S3	18.4 (15.2 – 22.4)
S4	16.8 (12.8 – 20.8)
S5	15.2 (12.0 – 19.2)

[1] Number of zero values indicated by Z

Table 5 | Structural and functional imaging characteristics. Data are presented as median (interquartile range). Supratentorial WMH volumes were obtained by semiautomatic segmentation of FLAIR images using a BINACA/LOCATE-based k-nearest neighbours algorithm and stratified by their distance to the lateral ventricles (<10 mm, periventricular; >10 mm, deep). Motion parameters were estimated during fMRIprep processing of BOLD scans. Fractional occupancies were calculated by assigning individual BOLD volumes to one of five discrete brain states defined by k-means clustering-based co-activation pattern analysis. Two high-occupancy states are labelled DMN+ and DMN- in view of their network connectivity profiles as shown in Figure 6.

	Estimate	P	95%-CI
Intercept	0.24	<0.0001	0.21 – 0.27
WMH, per 5.1-fold increase[1]	0.94	<0.0001	0.92 – 0.96
Age, per 10 years	1.04	0.001	1.01 – 1.06
Female sex	1.12	<0.0001	1.09 – 1.16
$\mathbf{1}_{\{WMH=0\}}$	0.93	0.477	0.75 – 1.14

[1] Interquartile ratio $2.37/0.468 = 5.06$

Table 7 | Association between time-spent in high-occupancy DMN-related brain states and WMH volume adjusted for age and sex. Beta regression table estimated from $n = 1651$ independent participants using the model equation $FO^{high} \sim \log WMH^+ + \mathbf{1}_{\{WMH=0\}} + age + sex$.

	Estimate	P	95%-CI
Intercept	53.41	< 0.0001	42.7 – 66.8
FO^{high}, per 5%	0.98	0.0116	0.96 – 0.99
WMH, per 5.1-fold increase[1]	1.01	0.367	0.98 – 1.05
Age, per 10 years	1.18	<0.0001	1.15 – 1.21
Female sex	0.99	0.666	0.95 – 1.03
Education, per year	0.97	<0.0001	0.97 – 0.98
$\mathbf{1}_{\{WMH=0\}}$	0.97	0.398	0.92 – 1.03

[1] Interquartile ratio $2.37/0.468 = 5.06$

Table 9 | Association between TMT-B and time spent in high-occupancy DMN-related brain states adjusted for age, sex, WMH volume and years of education. Gamma regression table estimated from $n = 1483$ independent participants using the model equation

$$TMT-B \sim FO^{high} + \log WMH^+ + \mathbf{1}_{\{WMH=0\}} + age + sex + educationyears.$$

540   # Supplementary results

541   ## Deep and periventricular WMH

542   Here we present, in analogy to Figure 5, the results of the multiverse analyses of
543   the association between cSVD burden, FO of DMN-related states, and executive
544   function, when cSVD is operationalized as the volume of deep or periventricular
545   white matter hyperintensities, respectively.
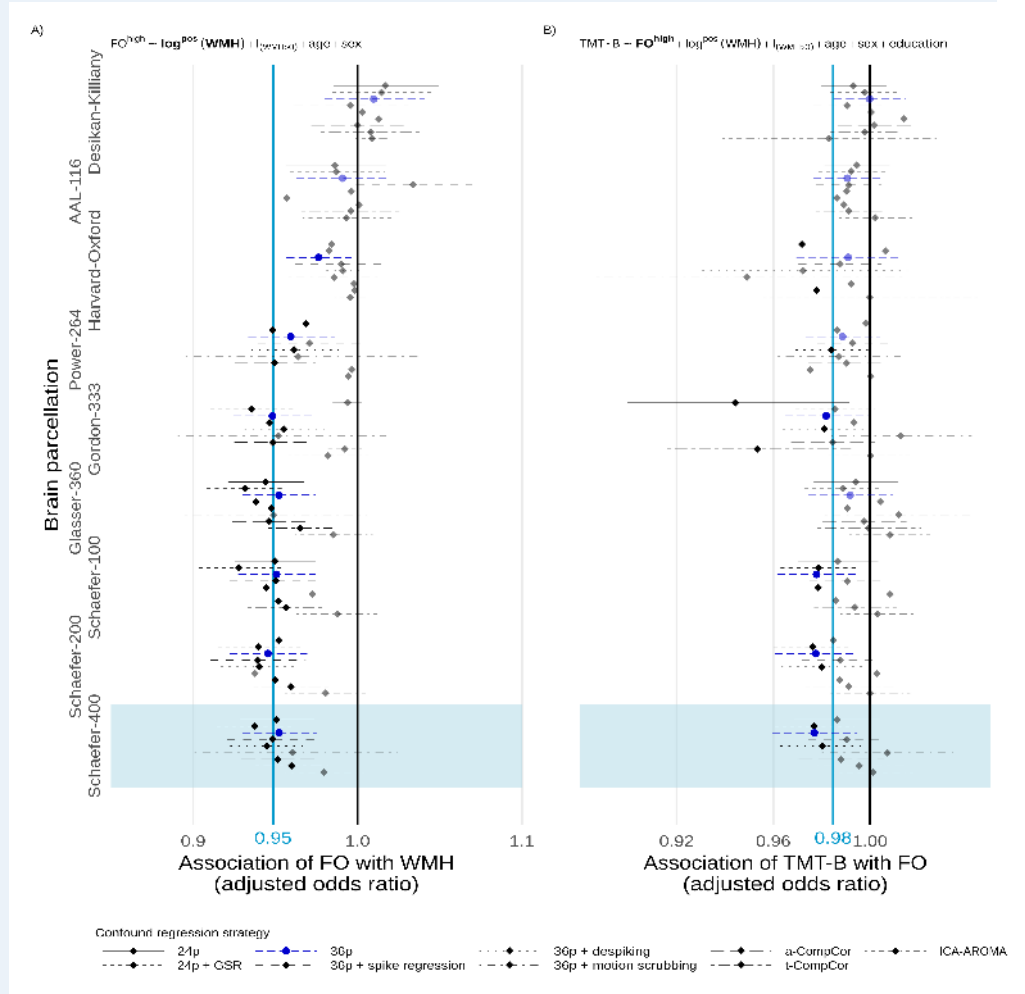
546
548   **Appendix 1—figure 1 Multiverse analysis, deep WMH**
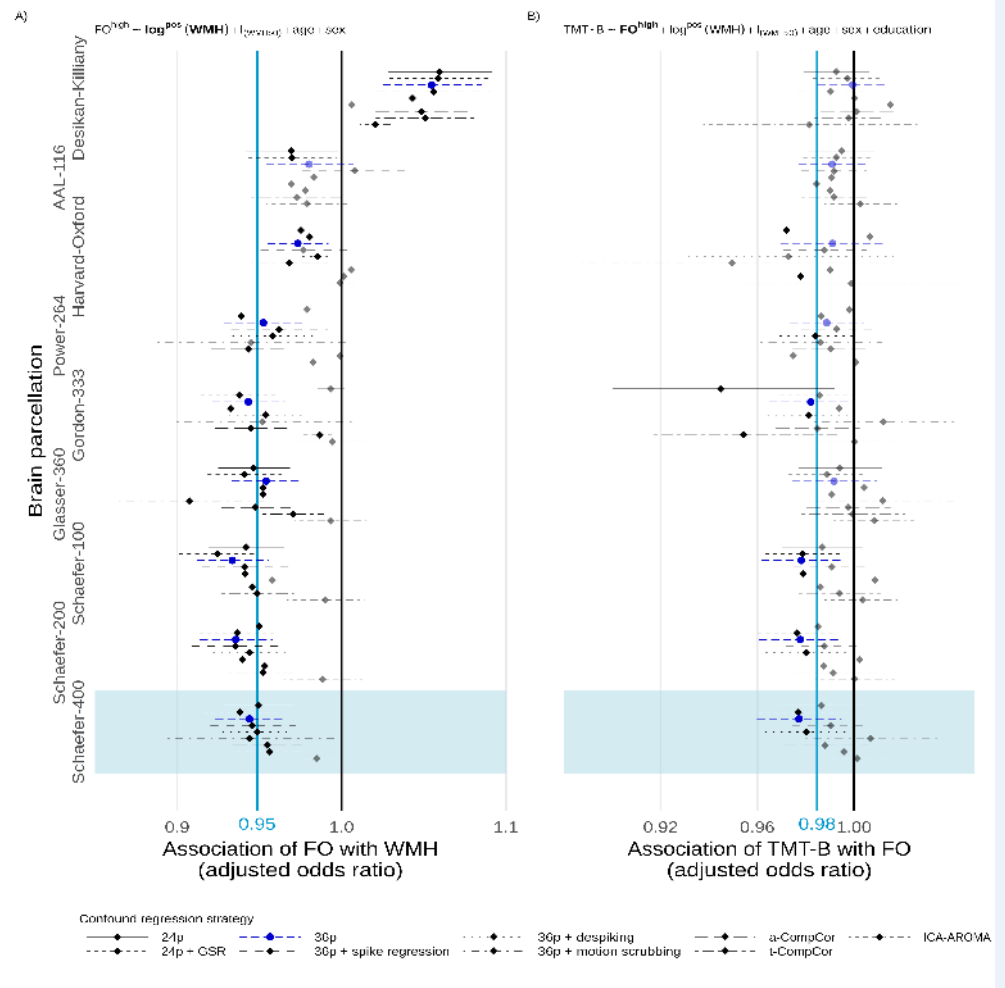
Appendix 1—figure 2 Multiverse analysis, periventricular WMH

Motion parameters

We also present, in analogy to Tables 7 and 9, regression tables for the association between time spent in DMN-related brain states (FO) and WMH volume, and between TMT-B and FO, adjusted for DVARS, RSMD and framewise displacement, in addition to age, sex and, in the latter case, years of education.

	Estimate	P	95%-CI
Intercept	0.32	<0.0001	0.28 – 0.36
WMH, per 5.1-fold increase[1]	0.96	0.0004	0.94 – 0.98
Age, per 10 years	1.01	<0.0001	1.00 – 1.01
Female sex	1.11	<0.0001	1.08 – 1.15
1{WMH=0}	0.91	0.3552	0.74 – 1.11

	Estimate	P	95%-CI
DVARS	0.98	<0.0001	0.98 – 0.99
RMSD	28.29	0.0055	2.67 – 299.84
Framewise displacement	0.16	0.0112	0.04 – 0.66

[1] Interquartile ratio 2.37/0.468 = 5.06

Appendix 1—table 2 Association between time-spent in high-occupancy DMN-related brain states and WMH volume adjusted for age, sex, and **motion parameters**

	Estimate	P	95%-CI
Intercept	46.83	<0.0001	36.74 – 59.72
FO^{high}, per 5%	0.71	0.0718	0.49 – 1.03
WMH, per 5.1-fold increase[1]	1.01	0.3414	0.98 – 1.04
Age, per 10 years	1.02	<0.0001	1.01 – 1.02
Female sex	1.00	0.8171	0.96 – 1.04
Education, per year	0.97	<0.0001	0.97 – 0.98
$1_{\{WMH=0\}}$	0.96	0.7581	0.73 – 1.29
DVARS	1.01	0.0001	1.00 – 1.01
RMSD	0.31	0.4695	0.01 – 7.45
Framewise displacement	1.08	0.9322	0.16 – 7.13

[1] Interquartile ratio 2.37/0.468 = 5.06

Appendix 1—table 4 Association between TMT-B and time spent in high-occupancy DMN-related brain states adjusted for age, sex, WMH volume and years of education, and **motion parameters**